6th Intercontinental Geoinformation Days

igd.mersin.edu.tr

Air pollution monitoring in Tehran using Sentinel_5 satellite (2022)

Nilufar Makky *[1], **Khalil Valizade Kamran** [1] **Sadra Karimzadeh** [1]

[1]University of Tabriz, Environmental Science, RSGIS, Tabriz, Iran

Keywords
Remote sensing
Air pollution
TROPOMI
Sentinel_5
Population

Abstract

Tehran is one of the biggest metropolises that has been affected by excessive pollution. People who are prone to heart disease and asthma should avoid traveling in areas with high pollution even if possible. Using Sentinel_5 (TROPOMI)sensor images, the amount of CO, NO_2, O_3, and Aerosol, which includes fine particles in the air, was checked and the density map of each of these parameters was created. By using these results, it is possible to identify excessively polluted areas and apply the necessary predictions for crisis management. Also, city temperature changes, construction and NDBI index can affect the amount of air pollution.

1. Introduction

The extent of climate change has already had significant impacts that can be seen in several dimensions. Managing climate challenges is very important for researchers. The average surface temperature of the Earth has been increased by about (1.62) degrees Fahrenheit since the late 19th century in all over the world (Boer et al., 2000; Kaufmann et al., 2011; Damtoft et al., 2008). Also, Air pollution is a very destroyer global crisis and it has a death toll of 7 million people per year, of which (600,000) of them are children (UN). In addition, Air pollution is a dangerous global threat that has many bad effects on human health and ecosystems. One of the most dangerous and toxic air pollutants is (NO2). It is responsible for respiratory diseases, cardiovascular diseases, reduced capacity of self-cleaning air the weakened immune function of the lungs, asthma, and many more (Srokzynski, 1988; WHO). According to the European Environment Agency (EEA), in 2018 year, 55,000 premature deaths from NO2 gas occurred across Europe (EEA). In addition, high nitrogen concentrations damage ecosystems due to eutrophication and acidification (along with sulfur dioxide, and SO2). This, in turn, leads to changes in the diversity of species (reduction in the level of existing species and invasion of new species) as well as an increase in the concentration of toxic metals in water and soil (Dopre et al, 2010). A major advance in satellite NO_2 observations was the TROPOSpheric Monitoring Instrument (TROPOMI), which was mounted on the Sentinel-5 Precursor (Sentinel-5P, S-5P) satellite launched by the European Space Agency. Atmospheric NO2 pollution has become even more threatening since the start of the COVID-19 pandemic, and many scientific studies have explained this. In this regard, a decrease in NO2 levels was reported in 2020. On a global and regional scale, they analyzed NO2 TVCD data in 33 cities worldwide, and only in more than 1 city (Isfahan) did atmospheric NO2 concentrations increase during the pandemic. The reason for this increase was ignoring the restrictions of COVID-19 in Iran (Bauwns et al, 2020). Fossil fuel CO2 emissions are mainly through the combustion of oil and coal, leading to climate change and disease in organisms globally (Li et al., 2021). O_3 is a gas often formed from NOx (nitrogen oxides) and hydrocarbons, released in the form of nanoparticles and ultra-fine particles with atmospheric contaminants (whether organic or inorganic). O_3 is released in large quantities by thermoelectric power plants and the internal combustion engines of motor vehicles, thus raising levels of atmospheric contamination on a global scale (Dong et al., 2021; Forest, 2021). Aerosols are compounds capable of containing high loads of atmospheric contaminants that spread over large regions, absorbing solar radiation, and leading to a greater imbalance in temperature in cities around the world (Mei et al., 2020; Fernandez-Moran et al., 2021; Bodah et al., 2022).

Today, energy consumption and air pollution are metropolitans' important transportation issues. In these

* **Corresponding Author**

*(nilufar_makky73@yahoo.com) ORCID ID xxxx – xxxx – xxxx – xxxx
(valizadeh@tabrizu.ac.ir) ORCID ID xxxx – xxxx – xxxx – xxxx
(sadra.karimzadeh@gmail.com) ORCID ID xxxx – xxxx – xxxx – xxxx

Cite this study

Makky, N, Kamran, K. V., Karimzadeh, S. (2023). Air pollution monitoring in Tehran using Sentinel_5 satellite (2022). Intercontinental Geoinformation Days (IGD), 6, 41-45, Baku, Azerbaijan

cities, most people consider their mode of transportation based on the appropriate means, including passenger, travel characteristics, population growth, urban space, and transportation (Bagheri et al,2020). Tehran is the most populated city in Iran its capital of it, has a population of 8.5 million, and this number reaches about 12.5 million people due to the daily commute of people who come from nearby cities such as Qom, Qazvin, and Karaj for work and education every day (Hosseini et al, 2016; Bayat et al, 2019) The other types of transportation in Tehran (smart modes, cycling, public transport) are marginal compared with the private mode in daily trips in Tehran city. In 2017, Tehran Traffic Organization information showed that the Tehran bus system was giving service to passengers by 10 BRT lines and 240 regular buses every day. Also, the important change in Tehran's urban transportation has been related to the metro, which started its operation in 1990. The information showed that in 2017, about 732 million trips were made by the metro in Tehran (Mojtehedzadeh et al, 2019).

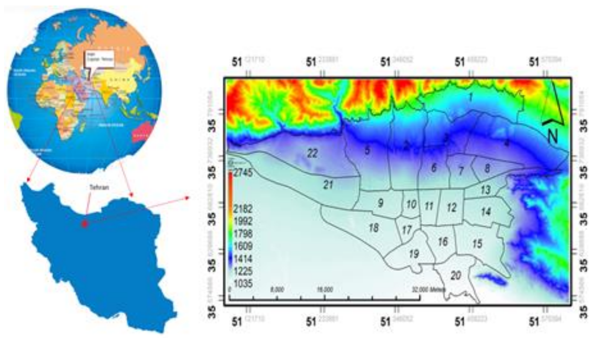

Figure 1. Tehran location

In this map, the elevation position of Tehran is displayed by The Shuttle Radar Topography Mission with a resolution of about 30 meters.

2. Method

Using remote sensing data to monitor air quality is important for environmental research. The Sentinel-5 satellite with the Tropomi sensor enables the tracking of gaseous pollutants. In this research, the TROPOMI sensor of the Sentinel 5 satellite was used to determine the number of suspended particles including NO_2, O_3, CO, and AEROSOL. All extracted gases have units based on mol/m^2 .The GEE environment was used for coding. The extracted maps were designed and displayed in ARC MAP 10.8 software.

3. Results

Nitrogen dioxide (NO_2) and nitrogen oxide (NO) together are commonly referred to as nitrogen oxides whose formula is ($NO_x = NO + NO_2$). They are the main trace gases in The Earth's atmosphere and are present in both the troposphere and the stratosphere layers. They are entering the atmosphere as a result of anthropogenic activities like (biomass burning and notably fossil fuel combustion) and natural processes (such as microbiological processes in soils, wildfires, and lightning). During the daytime, i.e., in the presence of sunlight, a photochemical cycle involving ozone (O_3) converts NO into NO_2 (and vice versa) on a timescale of minutes, so that NO_2 is a robust measure for concentrations of nitrogen oxides(tropomi.eu). The distribution map of NO_2 in Tehran city in 2022 and 2021 was shown in Figure 2.

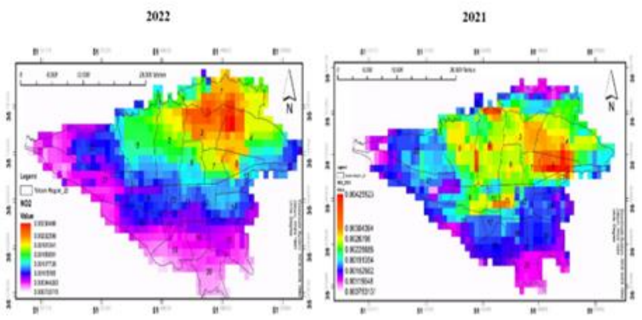

Figure 2. NO_2 distribution in Tehran

Also, Sentinel_5 provides near real-time high-resolution imagery of the UV Aerosol Index (UVAI), called the Absorbing Aerosol Index (AAI). The AAI is based on wavelength-dependent changes in Rayleigh scattering in the UV spectral range for a pair of wavelengths. The difference between observed and modeled reflectance results in the AAI. When the AAI is positive, it indicates the presence of UV-absorbing aerosols like dust and smoke. It is useful for tracking the evolution of episodic aerosol plumes from dust outbreaks, volcanic ash, and biomass burning(tropomi.eu). Here the map of Aerosol was shown in Figure 3.

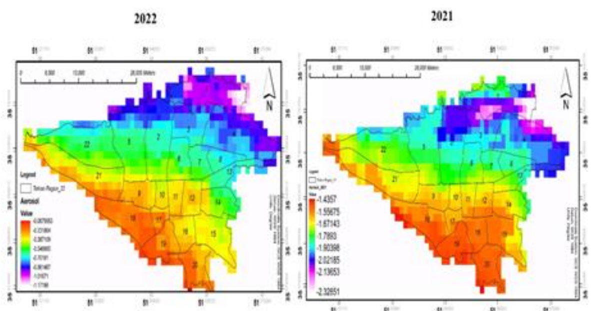

Figure 3. Aerosol distribution in Tehran

Carbon monoxide (CO) is an important atmospheric trace gas for understanding tropospheric chemistry. In certain urban areas, it is a major atmospheric pollutant. The main sources of CO are thecombustion of fossil fuels, biomass burning, and atmospheric oxidation of methane and other hydrocarbons. Whereas fossil fuel combustion is the main source of CO at northern mid-latitudes, the oxidation of isoprene and biomass burning play an important role in the tropics (tropomi. eu).

In the stratosphere, the ozone layer shields the biosphere from dangerous solar ultraviolet radiation. In the troposphere, it acts as an efficient cleansing agent, but at high concentrations, it also becomes harmful to the health of humans, animals, and vegetation. Ozone (O_3) is also an important greenhouse-gas contributor to ongoing climate change. Since the discovery of the Antarctic ozone hole in the 1980s and the subsequent Montreal Protocol regulating the production of chlorine-containing ozone-depleting substances, ozone has been routinely monitored from the ground and from space (tropomi.eu).

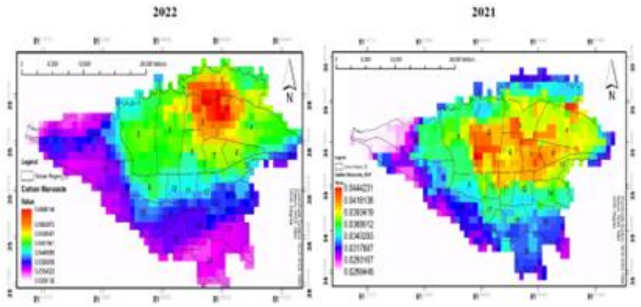

Figure 4. CO distribution in Tehran

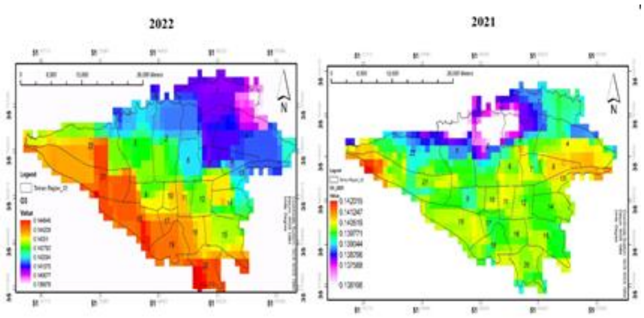

Figure 5. O_3 distribution in Tehran

Land surface temperature (LST) is one of the significant climatic parameters in energy balance and the state is controlled by the energy balance of the surface, atmosphere, thermal properties of the surface, and subsurface media (Utomo et al., 2017; Insan and Prasetya, 2021). LST can be interpreted as the average surface temperature of a surface depicted in the range of a pixel with various surface types. The formula here using to calculate LST (Rongali et al, 2011).

$$\text{LST} = \frac{BT}{1+(\lambda\,.\text{BT}/\rho\,)\ln\,\varepsilon} - 273.15$$

LST: Land surface temperature (in $°C$)

BT: At-satellite brightness temperature (in $°C$)

λ: Band 10 radiation wavelength (10,6 μm)

ρ: $(h.\ c)/\ \sigma$ (1,438 × 10−2 mK), where σ is Boltzmann constant, which value was 1,38 × 10−23 J/K;
h is Planck's constant whose value was 6,626 .10^{-34} Js; and c is the speed of light which value was 2,998 × 108 m/s ().

NDBI is used to extract built-up features of the city and the NDBI raster map is derived from the short-wave infrared (SWIR) and (NIR) channels of multiband remotely sensed imagery from Landsat8 in Gee (Garg et al.,2016). The formula for calculating NDBI is shown:

$$\textbf{NDBI} = \frac{(\boldsymbol{SWIR} - \boldsymbol{NIR})}{(\boldsymbol{SWIR} + \boldsymbol{NIR})}$$

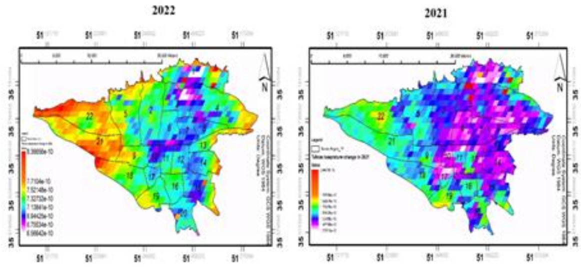

Figure 6. LST in Tehran

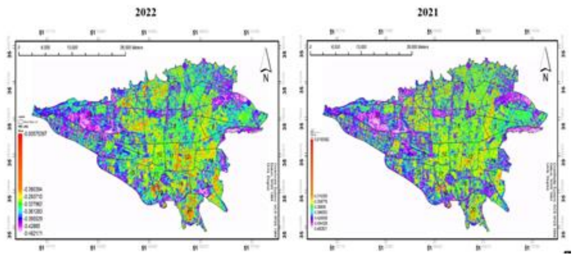

Figure 7. NDBI Index in Tehran

Vegetation indices based on visible and near-infrared bands have been widely used in vegetation detection and health assessments (Ke et al., 2015), among which the NDVI is most commonly used in vegetation-related monitoring. The definition of the NDVI is shown by Formula (Rouse et al., 2022):

$$\textbf{NDVI}\ (\boldsymbol{LANDSAT\_8}) = \frac{\boldsymbol{B5\_B4}}{\boldsymbol{B5} + \boldsymbol{B4}}$$

where *RED* (B4) is the reflectance in the red band and *NIR(B5)* is the reflectance in the near-infrared band. Different remote-sensing images have different NDVI formulae. The NDVI formulae for Landsat 8 L2 in this study used. The range of the NDVI is [−1,1]. (NDVI < 0 indicates that the ground cover is cloud, snow, water etc.); (NDVI=0 indicates that there are bare soil or rocks); and NDVI < 0 indicates that there is vegetation coverage, and the value increases with an increase in the coverage. The valid values of the NDVI were filtered, then only the pixel values with (NDVI ≥ 0) were kept (Zhao et al., 2023).

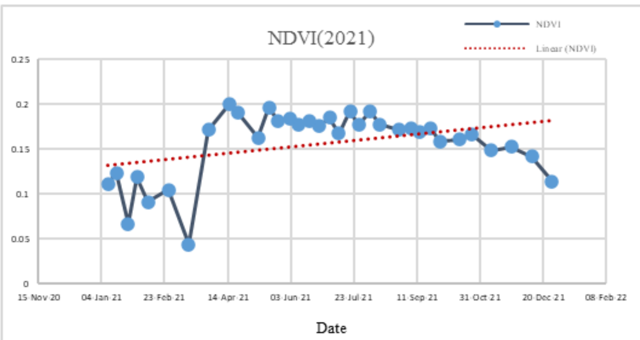

Figure 8. NDVI chart in 2021

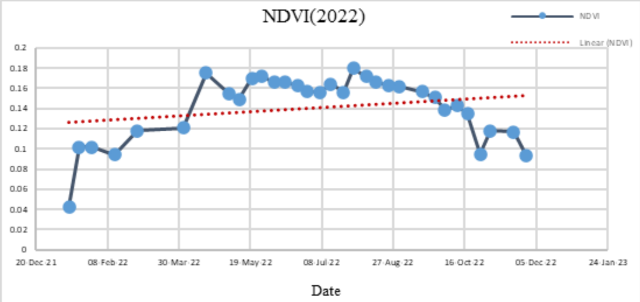

Figure 9. NDVI chart in 2022

4. Discussion

In this study, using remote sensing and the GEE system, our goal is to determine the areas prone to pollution in order to introduce people with respiratory diseases to maintain their health by not visiting these places.

5. Conclusion

In this research, the high-risk polluted areas in Tehran due to the presence of nitrogen dioxide, ozone, aerosols and carbon monoxide was extracted. According to the information obtained from the images of Sentinel 5, in 2021, the temperature of Tehran was lower than in 2022, and the increase in temperature, especially in areas 21 and 22, was minimized. Also, the NDVI index in 2021 provided a number of 0.193 for the health of the vegetation, but the maximum of this index in the year (2022) was 0.18, which indicates a decrease in the coverage and health of plants in the densely populated city of Tehran. Construction and urban density in 2022 compared to 2021 has grown significantly in regions (12, 16, 19, 20 and 4). The number of aerosols in the southern areas of Tehran has its maximum amount, but its amount has decreased relatively little in 2022. The amount of toxic carbon monoxide gas has reached its minimum in 2022 in regions 1, 3, and 4, and these regions are considered high risk. The presence of ozone gas is effective in preventing the penetration of high-energy ultraviolet rays, but its excessive increase in an area causes pollution. Ozone gas has increased in the south and southwest regions. Nitrogen dioxide gas has increased in regions 1, 3, and 4. It is harmful to identify places prone to pollution and not to visit these areas by people with respiratory diseases. The unit expressed for all particles is equal to (mol/m^2).

References

Bagheri, M., Ghafourian, H., Kashefioasl, M., Sadatipour, M. T., & Rabbani, M. (2023). Transport network traffic management and urban travel demand to reduce air pollution (Case study: Shiraz). International Journal of Nonlinear Analysis and Applications.

Bauwens, M., Compernolle, S., Stavrakou, T., Müller, J. F., Van Gent, J., Eskes, H., ... & Zehner, C. (2020). Impact of coronavirus outbreak on NO2 pollution assessed using TROPOMI and OMI observations. Geophysical Research Letters, 47(11), e2020GL087978.

Bayat, R., Ashrafi, K., Motlagh, M. S., Hassanvand, M. S., Daroudi, R., Fink, G., & Künzli, N. (2019). Health impact and related cost of ambient air pollution in Tehran. Environmental research, 176, 108547.

Boer, E. P. J., & Hendrix, E. M. (2000). Global optimization problems in optimal design of experiments in regression models. Journal of Global Optimization, 18, 385-398.

Damtoft, J. S., Lukasik, J., Herfort, D., Sorrentino, D., & Gartner, E. M. (2008). Sustainable development and climate change initiatives. Cement and Concrete Research, 38(2), 115–127.

Duprè, C., Stevens, C. J., Ranke, T., Bleeker, A., Peppler-Lisbach, C. O. R. D., Gowing, D. J., ... & Diekmann, M. (2010). Changes in species richness and composition in European acidic grasslands over the past 70 years: the contribution of cumulative atmospheric nitrogen deposition. Global Change Biology, 16(1), 344-357.

European Environment Agency. Air Quality in Europe—2020. Report. EEA Report No 9/2020. Available online: https://www.eea.europa.eu/publications/air-quality-in-europe-2020-report (accessed on 10 October 2021).

Garg, A., Pal, D., Singh, H., & Pandey, D. C. (2016, November). A comparative study of NDBI, NDISI and NDII for extraction of urban impervious surface of Dehradun [Uttarakhand, India] using Landsat 8 imagery. In 2016 International Conference on Emerging Trends in Communication Technologies (ETCT) (pp. 1-5). IEEE.

Hosseini, V., & Shahbazi, H. (2016). Urban air pollution in Iran. Iranian Studies, 49(6), 1029-1046.

http://www.tropomi.eu/data.products

https://ntrs.nasa.gov

Insan, A. F. N., & Prasetya, F. A. S. (2021). Sebaran Land Surface Temperature Dan Indeks Vegetasi Di Wilayah Kota Semarang Pada Bulan Oktober 2019. Buletin Poltanesa, 22(1), 45-52.

Kaufmann, R. K., Kauppi, H., Mann, M. L., & Stock, J. H. (2011). Reconciling anthropogenic climate change with observed temperature 1998–2008. Proceedings of the National Academy of Sciences, 108(29), 11790–11793.

Ke, Y., Im, J., Lee, J., Gong, H., & Ryu, Y. (2015). Characteristics of Landsat 8 OLI-derived NDVI by comparison with multiple satellite sensors and in-situ observations. Remote sensing of environment, 164, 298-313.

Li, M., Liu, W., Liu, W., Bi, M., & Cui, Z. (2021). Dynamic substance flow analysis of lead in the fossil fuel system of China from 1980 to 2018. Journal of Cleaner Production, 313, 127918.

Mojtehedzadeh, M. (2019) Assessment of Urban Transport System in Tehran. Suti Report; United Nation Economic and Social Commission for Asia and Pacific (ESCAP): Bangkok, Thailand.

Rongali, G., Keshari, A. K., Gosain, A. K., & Khosa, R. (2018). A mono-window algorithm for land surface temperature estimation from Landsat 8 thermal infrared sensor data: a case study of the Beas River Basin, India. Pertanika J Sci Technol, 26(2), 829-840.

Rouse, J. W., Haas, R. W., & Schell, J. A. (2022). Monitoring the Vernal Advancement and Retrogradation (Greenwave Effect) of Natural Vegetation. NASA/GSFCT Type III Final Report.

Sroczyński, J. (1988). The Impact of Atmos. In Air Pollution on Human Health; PAN: Wrocław, Poland. (In Polish)

UN. With a Premature Death Every Five Seconds, Air Pollution Is Violation of Human Rights. online: https://www.un.org/sustainabledevelopment/with-a-premature-death-every-five-seconds-air-pollution-is-violation-of-human-rights-says-un-expert-2/

Utomo, A. W., Suprayogi, A., & Sasmito, B. (2017). Análisis hubungan variasi land surface temperature dengan kelas tutupan lahan menggunakan data citra satelit landsat (Studi Kasus: Kabupaten Pati). Jurnal Geodesi Undip, 6(2), 71-80.

Veefkind, J. P., Aben, I., McMullan, K., Förster, H., De Vries, J., Otter, G., ... & Levelt, P. F. (2012). TROPOMI on the ESA Sentinel-5 Precursor: A GMES mission for global observations of the atmospheric composition for climate, air quality and ozone layer applications. Remote sensing of environment, 120, 70-83.

World Health Origination (WHO) Air Quality Guidelines for Particulate Matter, Ozone, Nitrogen Dioxide and Sulfur Dioxide. Available online: https://apps.who.int/iris/handle/10665/345329

Zhao, Y., Hou, P., Jiang, J., Zhao, J., Chen, Y., & Zhai, J. (2023). High-Spatial-Resolution NDVI Reconstruction with GA-ANN. Sensors, 23(4), 2040.